

Evidence of mixed phases and percolation at the metal-insulator transition in two dimensions.

Shiqi Li, Qing Zhang, Pouyan Ghaemi, and M. P. Sarachik

Department of Physics, City College of New York,

160 Convent Ave., New York, New York 10031, USA

CUNY Graduate Center, 365 Fifth Avenue, New York, New York 10016, USA

(Dated: September 1, 2021)

The in-plane magnetoconductance of the strongly interacting two-dimensional electron system in a silicon MOSFET (metal-oxide-semiconductor-field-effect transistor) exhibits an unmistakable kink at a well-defined electron density, n_k . The kink at n_k is near, but not at the critical density n_c determined from resistivity measurements, and the density at which n_k occurs varies with temperature. These features are inconsistent with expectations for a quantum phase transition. We suggest instead that this is a percolation transition and present a detailed model based on the formation of a mixed insulating and metallic phase within which a metal-insulator transition takes place by percolation.

PACS numbers:

INTRODUCTION

Based on the famous 1979 paper by Abrahams *et al.* [1], as well as several carefully executed experiments on different materials, it was assumed for many years that a metal-insulator transition cannot occur and no metallic phase can exist in a two-dimensional electron/hole system. It was therefore a surprise when experimental studies in the 1990's appeared to show that such a transition does take place in low disorder, dilute two-dimensional (2D) electron systems when strong electron interactions rather than the kinetic energy are dominant and determine the behavior of the system [2–4]. In addition to the dramatic change in resistivity that signals the onset of a conducting phase, unusually interesting behavior was found for the magnetoresistance both above and below the critical electron density n_c . On both sides of the transition, the resistivity rises sharply with increasing in-plane magnetic field up to a field B_{sat} , above which it becomes essentially constant. Shubnikov-de Haas measurements [5–7] have demonstrated that B_{sat} signals the onset of full polarization of the electron spins.

A great deal of discussion ensued concerning these experimental observations: is this a true quantum phase metal-insulator transition, which many believed cannot occur in two dimensions, or can be explained within any one of a number of relatively benign scenarios. (For reviews, see Refs. [8–10].)

While abrupt changes and divergences have been reported at n_c for a variety of physical properties [8–11], the benign behavior of the magnetoresistance at the critical electron density has been an enigma since its discovery [12, 13]. While the resistivity displays a sharp change as one crosses the transition at the critical density, the magnetoresistance appears to vary smoothly without exhibiting any change that would signal the onset of a new phase [14].

In this paper we report the results of detailed measurements of the magnetoresistance of a two-dimensional low-disorder, dilute, strongly interacting system of electrons in a silicon metal-oxide-semiconductor-field-effect transistor (MOSFET) over a broad range of electron densities. Despite the striking similarity of the magnetoconductance in the metallic and insulating phases and the gradual evolution of the behavior found to date as the transition is crossed, we report that the in-plane field B_{sat} required to fully polarize the electron spins exhibits an abrupt kink as a function of electron density that signals the occurrence of a transition at a well-defined density n_k that varies with temperature and is near, but not at, the density n_c for the metal-insulator transition determined from resistivity measurements. These features are inconsistent with the behavior expected for a quantum critical transition. We propose instead that the kink signals the occurrence of a transition by percolation within a mixed metallic-insulating phase.

EXPERIMENTAL PROCEDURE

Measurements were performed down to 0.27 K in an Oxford Heliox He-3 refrigerator on the same type of high-mobility silicon MOSFET samples as those used in previous studies [11, 15]. Here we report data taken for a sample with critical density $n_c \approx 7.74 \times 10^{10} \text{ cm}^{-2}$ in the absence of magnetic field and $\approx 9.0 \times 10^{10} \text{ cm}^{-2}$ in a field sufficient to fully polarize the electron spins [15]. Contact resistance was minimized by using a split-gate geometry which permits high electron density to be maintained near the contacts independently of the value of the electron density in the main part of the sample. This is a particularly important feature that enables reliable measurements in the dilute 2D electron system in the deeply insulating state where the resistivity reaches

very high values. By contrast with the lock-in techniques that were sufficient for our earlier measurements of higher density, metallic-like samples that have relatively low resistivities [16], the measurements here were taken by a protocol similar to that described in Ref. [15], where a Keithley Source Measure Unit SMU 236 was used to apply a small dc current (as low as a few pA) through the sample and the voltage was measured by a standard four-probe method. For each density and temperature, the resistivity ρ was deduced from the slope of the linear portion of the corresponding I - V characteristic, as shown in the upper inset to Fig. 1.

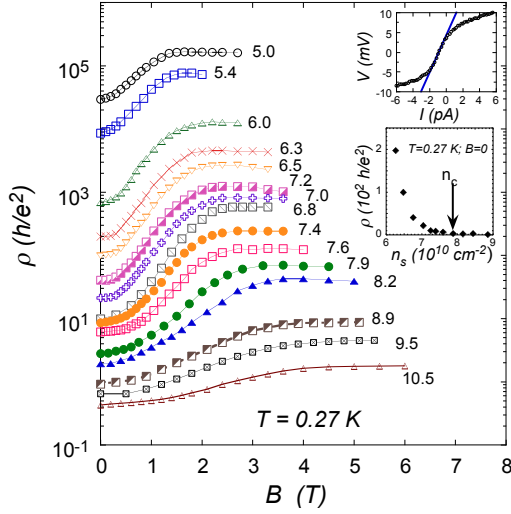


FIG. 1: The resistivity as a function of parallel magnetic field at $T = 0.27$ K plotted on a semilogarithmic scale for different electron densities (in units of 10^{10} cm^{-2}), as labeled. The small decrease of the resistance in some of the curves for magnetic fields above saturation is due to minor misalignment of the field away from the in-plane direction. Upper Inset: The resistivity deduced from the slope of the linear portion of the corresponding I - V characteristic for each density and temperature; here $T = 0.27$ K, $B = 0$ T; $n_s \approx 4.7 \times 10^{10} \text{ cm}^{-2}$. Lower inset: A plot of ρ as a function of electron density n_s illustrates the abrupt change in resistivity at n_c .

EXPERIMENTAL RESULTS

For various different electron densities, Fig. 1 shows the resistivity at $T = 0.27$ K as a function of magnetic field applied parallel to the plane of the sample. In agreement with data shown in earlier reports [14], the in-plane magnetoconductance rises dramatically with increasing magnetic field and reaches a plateau above a density-dependent field B_{sat} . The behavior of the magnetoconductance is qualitatively the same in the insulating phase as

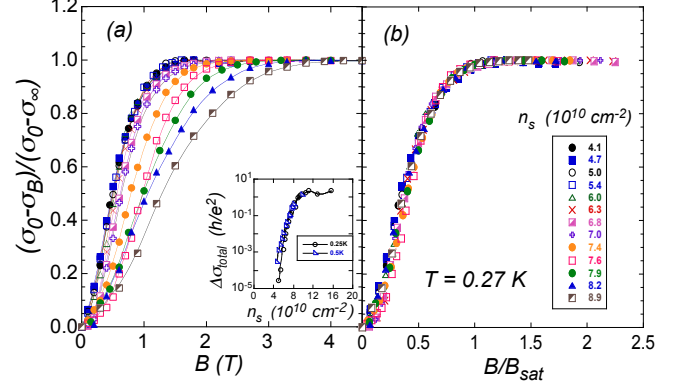


FIG. 2: (a) Normalized conductivity as defined by Eq. (1) plotted as a function of in-plane magnetic field B ; $T = 0.27$ K. The inset shows $\Delta\sigma_{total} = [\sigma(B=0) - \sigma(B \rightarrow \infty)]$ versus electron density n_s . (b) Normalized conductivity as a function of B/B_{sat} , where the fitting parameter B_{sat} was chosen to yield a collapse of the normalized conductivity onto a single curve.

it is in the conducting phase and appears to evolve continuously and smoothly, with no indication that a transition has been crossed. As shown in the lower inset of Fig. 1, this is in clear contrast with the dramatic change found for the zero-field resistance as the electron density is reduced below n_c , a change that becomes sharper and more pronounced as the temperature is reduced into the milli kelvin range.

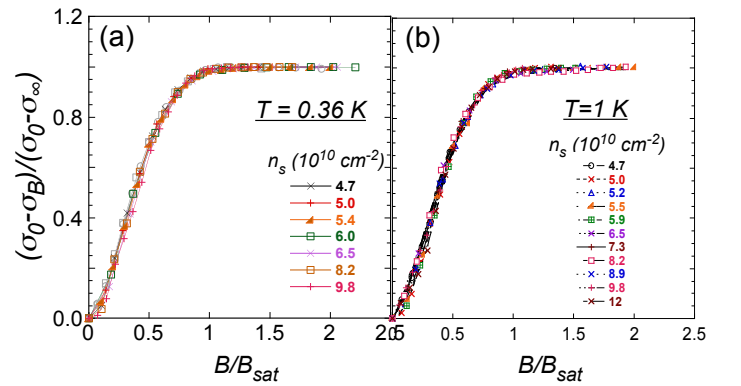


FIG. 3: To illustrate the collapse obtained at each (constant) temperature, the normalized conductivity is shown as a function of B/B_{sat} at two temperatures above base: (a) 0.36 K; (b) 1.0 K.

Following the procedure used in a previous study [16], we determine the normalized magnetoconductivity:

$$\sigma_{\text{norm}} \equiv \frac{\sigma(B=0) - \sigma(B)}{\sigma(B=0) - \sigma(B \rightarrow \infty)} = \frac{\Delta\sigma}{\Delta\sigma_{total}}. \quad (1)$$

Note that the normalized magnetoconductivity is sim-

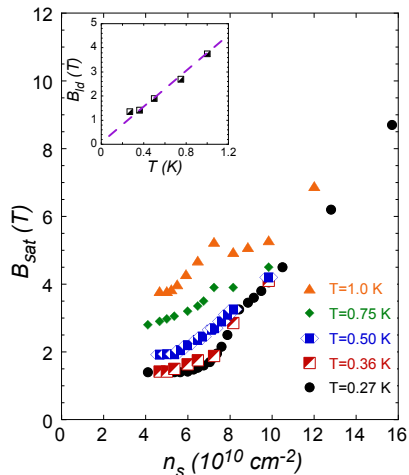


FIG. 4: B_{sat} as a function of electron density for different temperatures, as labeled. The inset shows the terminal, low-density value of B_{sat} as a function of temperature.

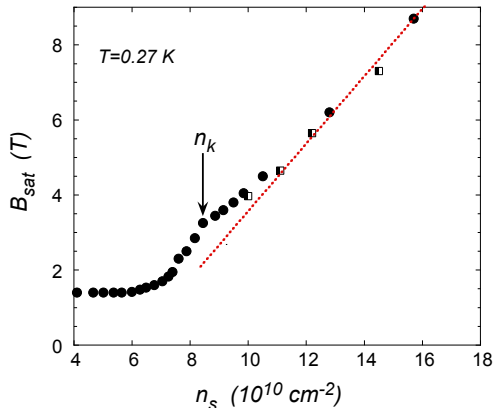


FIG. 5: B_{sat} as a function of n_s at base temperature. The closed circles are for the sample for which most of the data were obtained, while the half-open squares were obtained for a similar sample with a different value of n_c (see the Appendix). To aid the discussion in the text, the dotted line is an approximate straight line fit to the high density values, extended to lower densities.

ply the field dependent contribution to the conductivity, $\Delta\sigma = [\sigma(B = 0) - \sigma(B)]$, normalized by its full value, $\Delta\sigma_{total} = [\sigma(B = 0) - \sigma(B \rightarrow \infty)]$.

Figure 2 (a) shows the normalized conductivity at $T = 0.27$ K as a function of in-plane magnetic field for different electron densities. The inset is a plot of $\Delta\sigma_{total} = [\sigma(B = 0) - \sigma(B \rightarrow \infty)]$ as a function of electron density. Notwithstanding the apparent continuity of the behavior of the magnetoconductance across the tran-

sition, the inset shows that there is a sharp change in the magnetoconductivity in the vicinity of a critical density n_c .

As shown in Fig. 2(b), a density-dependent parameter can be chosen that provides a collapse onto a single curve for all the data obtained at base temperature; note that the scale of B_{sat} was chosen such that the onset of saturation occurs at $x = 1 = B/B_{sat}$. Data were also taken at 0.36, 0.50, 0.75 and 1.0 K. Figure 3 illustrates that the B_{sat} obtained at 0.36 and 1.0 K are also self-similar and collapse onto a single curve (data for 0.5 and 0.75 K not shown).

Figure 4 shows a plot of B_{sat} for a broad range of electron density at five different low temperatures. A clear kink occurs at a density (that varies with temperature), below which B_{sat} decreases with decreasing electron density and assumes a constant terminal value, B_{ld} . The inset shows a plot of the constant terminal value of B_{ld} as a function of temperature. To aid the discussion below, B_{sat} at the base temperature ($T = 0.27$ K) is shown separately in Fig. 5.

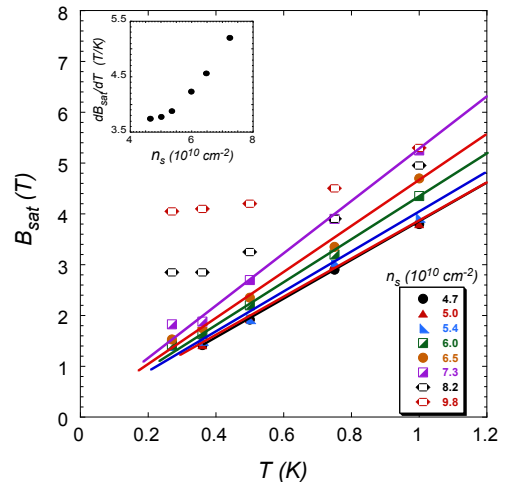


FIG. 6: B_{sat} as a function of temperature T . For the six lower densities, which are insulating, the lines are linear fits to the data not including the data at the lowest temperature $T = 0.27$ K, which lie above the curve. The upper two curves are on the metallic side of the transition. The inset shows the slope A of the B_{sat} vs. T curves in the insulating phase as a function of electron density.

Figure 6 shows B_{sat} as a function of the temperature T for various different electron densities. For each of the six densities on the insulating side of the transition, B_{sat} is consistent with the linear fits shown. Thus, $B_{sat} = AT$. Note that the lowest temperature points all deviate upward from the straight lines. Although we ascertained that the resistance of the sample exhibited exponential (variable-range-hopping) behavior down to base temper-

ature, it is possible that the electron system was not thermally well connected to the bath at our lowest temperatures. More densely spaced data taken at lower temperatures are needed to determine whether B_{sat} tends to zero in the limit of zero temperature. By contrast, B_{sat} extrapolates to a finite value at $T = 0$ for the two highest (metallic) densities, signaling the entry into a different phase. For the insulating phase, the inset shows that the slope A of the straight line fits as a function of electron density decreases as the density is reduced and levels off to a constant value.

DISCUSSION

In this paper we report measurements of the resistivity as a function of in-plane magnetic field in the strongly interacting two-dimensional electron system in a silicon MOSFET over a broad range of electron densities spanning the insulating and metallic phases at several temperatures below 1 K. Plotted as a function of in-plane magnetic field, B , the normalized conductivity defined by Eq. (1) then yields a set of self-similar curves that can be collapsed onto a single curve for all measured electron densities and temperatures using a parameter B_{sat} , where B_{sat} is the in-plane magnetic field required to fully polarize the electron spins in the system. B_{sat} is found to exhibit surprising, complex and interesting behavior as shown in Figs. 4 and 5. We call attention to the following notable features:

(A) While B_{sat} follows the straight line behavior expected for a Fermi liquid at high electron densities (see the dotted red line in Fig. 5), there is a clear upward deviation from the straight line as the electron density approaches a kink.

(B) Shown by the arrow in Fig. 5, there is an unmistakable kink at a well-defined density n_k followed by an abrupt decrease of B_{sat} as the electron density is further reduced. The kink at n_k signals the occurrence of a transition at a density that coincides with neither the zero-field critical density n_c nor its value in a magnetic field. It occurs at finite temperature and its position varies with temperature.

(C) As the electron density is decreased into the insulating phase, the saturation magnetic field B_{sat} decreases and reaches a constant, limiting value B_{ld} at low electron density, with a limiting value B_{ld} that depends on temperature.

As we will argue below, these features are consistent with a model that considers mixed metallic and insulating phases near the metal-insulator transition provided that the insulating component is the phase with the lower electron density. Indeed, local measurements of the compressibility by Ilani *et al.* [17] in the interacting GaAs-based 2D system have demonstrated the presence of an admixture of microscopic fractions of different phases.

Suggestions for such mixed phases include an insulating component associated with a disorder potential [18], the formation of insulating inclusions due to density inhomogeneities [19], the formation of insulating Wigner crystallites in a Fermi sea of electrons [20], a non-Fermi-liquid two-phase state involving non-conducting spin droplets [21, 22], and mesoscopic fluctuations [23].

High-density region

At high densities the two-dimensional electron gas is in a Fermi-liquid phase and the saturation magnetic field corresponds to the Zeeman field that fully polarizes the spin of all the electrons corresponding to a Zeeman field that is of the order of the Fermi energy. As a result, the saturation magnetic field at high densities varies linearly with the total density. As the electron density is reduced toward the kink, regions of an insulating phase begin to form. Since the insulating regions have density lower than the remaining Fermi-liquid regions (with correspondingly lower saturation field), their density will be smaller than the average density. The density of the remaining Fermi-liquid regions will therefore be larger than the average density (corresponding to higher saturation field). As discussed explicitly in Appendix B, the conductivity of the sample is determined mainly by the properties of parallel paths through the Fermi-liquid which have much higher conductance than the parallel paths through insulating regions. As a result, B_{sat} is determined largely by the conduction through the Fermi-liquid regions. Since the electron density of Fermi-liquid regions is higher than the average density, B_{sat} shows an upward deviation as the average density is decreased.

The KINK - A transition by percolation

The upturn from linear dependence continues until the percolation limit is reached. At this point, due to the increase of the volume fraction of insulating regions, there no longer exists an uninterrupted path for the electrons to travel through the Fermi-liquid regions. All the paths connecting the two edges through the Fermi liquid are now blocked by insulating regions and the (much lower) conduction proceeds by hopping [15]. At these densities, the Fermi-liquid and insulating regions act as resistances in series, and the conductivity of the sample is thus mainly determined by the lower conductivity of the insulating regions. The insulating regions have much lower saturation magnetic fields and the percolation transition thus leads to a sharp drop of the saturation magnetic field.

In a nutshell, the conduction at densities above the kink depends overwhelmingly on the conductivity of the Fermi-liquid regions which have higher than average den-

sity, while the conduction below the kink depends mainly on the conductivity of the insulating regions, which have lower than average density. Since the conductivity of the Fermi-liquid and insulating regions affect the density in fundamentally different ways, the saturation magnetic field measured through conductance shows the abrupt kink in Fig. 4.

The kink occurs at finite temperature, its density, n_k , changes with temperature, and n_k is not the same as either the critical density n_c or its value in a magnetic field. In fact, the electron density at which the kink occurs varies with temperature; we expect that its position will depend on the temperature dependence of the volume distribution of insulating and metallic regions. A major implication is that this transition is not the same as the famous quantum phase transition that has been claimed on the basis of numerous measurements in many different dilute two-dimensional strongly interacting systems [8–11]. Instead, we suggest it is a percolation transition that occurs within a mixed phase system.

It should be noted that a percolation transition has been claimed by a number of investigators, including He and Xie [18] who proposed a percolation transition due to the disorder landscape below a liquid-gas critical temperature; Meir [24] who suggested a percolation transition due to finite dephasing time at low temperature; and Das Sarma and co-workers [19, 25] who advocated a density inhomogeneity driven percolation transition due to the breakdown of screening in the random charged impurity disorder background.

Low-density region

Clearly shown in Fig. 4, the saturation field B_{sat} decreases as the density is reduced below n_k and becomes constant at a temperature-dependent low-density value B_{ld} that decreases with decreasing temperature. The inset to the figure shows the low-density B_{ld} versus temperature T . Based on the few points available, B_{sat} goes linearly to zero at $T = 0$. By the same token, Fig. 6 shows that B_{sat} is a linear function of temperature that is consistent with $B_{sat} \rightarrow 0$ at $T = 0$. As noted earlier, more densely spaced data taken at lower temperatures are needed to determine whether B_{sat} tends to zero in the limit of zero temperature. The slope of these curves decreases with decreasing density and saturates to a constant value, as shown in the inset. The fact that B_{sat} versus temperature becomes independent of the electron density at very low densities implies that in this regime the magnetoresistance is associated with non-interacting electrons that respond to the externally applied magnetic field individually and independently. That the slope of the curves deviates from this terminal value as the electron density is increased may be due to the onset of electron-electron interactions. The limiting value of the

slope is the same as the temperature dependence of saturation magnetic field for the polarization of single electrons. This feature indicates that the conductivity at lowest densities is by noninteracting low-density excited electrons at temperatures well below the Fermi temperature.

A quantum phase transition manquée

Based on our measurements and analysis of the magnetoconductance of strongly interacting electrons in 2D in a high-mobility silicon MOSFET, we suggest that the system is headed toward a phase transition between an insulating phase at low density where $B_{sat} \rightarrow 0$ in the limit of zero temperature and a metallic phase at higher electron density where B_{sat} remains finite as $T \rightarrow 0$. However, the system becomes unstable as the critical point is approached and separates instead into a mixture of component phases of a nature that has yet to be determined. Rather than approaching a quantum critical point as the electron density is varied and the temperature is reduced toward $T = 0$, the system develops mixed conducting/insulating phases where a metal-insulator transition occurs by percolation.

Comparison with earlier work

The kink we report in this paper was not observed in any of the earlier magnetotransport measurements of B_{sat} as a function of electron density [16, 26–33]. While a few papers included data for insulating electron densities [31], most of these earlier measurements were obtained for densities on the metallic side of the transition. Measurements in GaAs-based systems by Yoon *et al.* [26] and in high-mobility SiGe by Lu *et al.* [33] yielded results that are in clear disagreement with ours. It is possible that the results we have obtained require some degree of disorder (not too much, not too little), and that no mixed phases are formed in the limit of zero disorder.

Based on measurements of B_{sat} as a function of metallic electron densities in silicon MOSFETs, our group [16] and contemporaneous work of Shashkin *et al.* [27] inferred that B_{sat} extrapolates to zero at a finite critical density n_c , implying that there is a ferromagnetic instability and a quantum phase transition at that density. By tracing B_{sat} carefully through the transition region, we have now shown that, rather than going to zero as assumed earlier, B_{sat} remains finite (it actually exhibits a kink). This implies that there is no instability and no divergence (at least at finite temperature), and thus no evidence for ferromagnetism in this system, in agreement with recent measurements of Pudalov *et al.* [34].

SUMMARY AND CONCLUSIONS

We have shown that the in-plane magnetic field required to fully polarize the electrons in a strongly interacting electron system in two dimensions exhibits a clear, heretofore unobserved, kink as a function of electron density. On the basis of our data and analysis, we suggest that the behavior of the 2D electron system in silicon MOSFETs is consistent with a finite-temperature percolation transition within a mixed electronic phase.

Our results are novel and important, and promise to open new avenues of investigation using the behavior of the magnetoconductance as a tool. In particular, more data at much lower temperatures are needed to determine the position of the kink, n_k , as the temperature, magnetic field and disorder are varied, and to investigate the relation of n_k to the critical density, n_c , of the metal-insulator transition determined from measurements of the resistivity, thermopower, magnetic response, and other experimental probes.

APPENDIXES

Appendix A

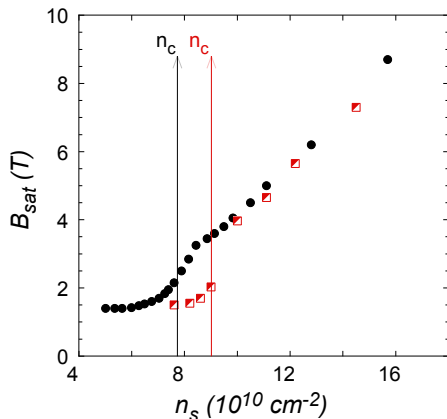


FIG. 7: Comparison between B_{sat} at $T = 0.27$ K (black dots) for the sample currently under study and B_{sat} deduced from the conductivity data in Fig.1(b) in Ref. [29](red open squares); the vertical lines show the two different critical densities n_c explicitly.

It is illuminating to consider a cross comparison between the data obtained for this sample with similar data obtained earlier for a sample of lower mobility and a higher level of disorder and higher critical density $n_c \approx 9.0 \times 10^{10} \text{ cm}^{-2}$ (compared to $n_c \approx 7.74 \times 10^{10} \text{ cm}^{-2}$). Shown in Fig. 7, the square (round) symbols denote the results for the sample with higher (lower) critical density. The points overlap nicely in the insulating

and metallic phase far from n_c . Not surprisingly, however, the behavior of B_{sat} near n_c is shifted to reflect the different values of the critical concentration. Clearly, the critical behavior associated with the metal-to-insulator transition simply shifts as the critical density shifts to lower densities for lower disorder samples, leaving the behavior far from the transition intact. This needs to be kept in mind whenever a comparison is made between different samples.

Appendix B

The general features of the model we propose rely solely on the development with decreasing electron density of a mixed phase composed of a Fermi liquid (or gas) and an insulating component of lower electron density than the liquid. In order to understand the origin of the kink in B_{sat} versus the electron density n_s , we need to examine the nature of the conductivity over the entire range of electron densities, both above and below the kink.

Many techniques have been used to calculate the conductivity of composite conductors [35]. The model we propose below applies to any mixture of a conducting and an insulating phase provided that the insulating phase has the smaller electron density. For specificity, we choose to consider an electronic microemulsion composed of insulating Wigner crystals and a conducting Fermi liquid, as suggested by Spivak and Kivelson [20, 36]. We propose a simplified model that captures the essential effect of the geometry of the crystalline and liquid regions on the measured saturation field.

We consider the sample to be a rectangle with width D perpendicular to the direction of the current and length L along the direction of current. We assume the effective length of the Fermi-liquid and Wigner crystal regions are l_F and l_W and their effective widths are d_F and d_W , respectively. At large densities, B_{sat} decreases linearly with the decrease of density, the behavior expected for a Fermi liquid. As the density is decreased toward n_k , the Wigner crystal regions start to emerge in the parent Fermi liquid. The Wigner crystal regions have insulating behavior but the sample presents conducting behavior so long as the Fermi-liquid regions are large enough to percolate between the two edges. Assuming that the length of the Fermi and Wigner regions are of the order of the sample length, the conductance is through parallel Fermi-liquid and Wigner crystal regions connecting the two ends of the sample. The effective conductivity of the sample will then be:

$$\sigma = \sigma_F \frac{d_F}{D} + \sigma_W \frac{d_W}{D} \quad (2)$$

where σ_W and σ_F are the conductance of Wigner crystal

and Fermi liquid, respectively. Since $\sigma_W \ll \sigma_F$, and assuming that for densities above n_k the Wigner crystal regions are not much larger than the Fermi-liquid regions ($d_w \gg d_F$), Eq. (2) gives $\sigma \approx \sigma_F \frac{d_F}{D}$ and the normalized conductivity in Eq. (1) reads

$$\sigma_{norm}(B) \approx \frac{\Delta\sigma_F}{\Delta\sigma_{F,Tot}} = \sigma_{norm}^F(B). \quad (3)$$

Thus, for densities above n_k , the saturation magnetic field corresponds to that of the Fermi liquid. It is important to understand how the emergence of Wigner crystal regions affect the density in the remaining Fermi liquid. Since Wigner crystals have a lower density than the parent Fermi liquid, their formation causes the density of the remaining liquid to increase, with a consequent deviation of B_{sat} upward from straight line behavior as the kink is approached from above. Figures 4 and 5 show such an increase of B_{sat} versus total density n_s as the density is decreased toward the kink.

As the density is decreased further, the fraction of the Wigner crystal regions increases and, ultimately, there will be no path through the Fermi-liquid regions to connect the two edges of the sample. We suggest that the appearance of the kink at the density n_k corresponds to a percolation transition. At densities below n_k , the paths connecting the two edges of the sample pass through Wigner crystal and Fermi-liquid regions in series. The effective conductivity of the sample is then given by

$$\sigma = \frac{L}{D} \frac{\sigma_F \sigma_W d_F}{\sigma_F l_W + \sigma_W l_F}. \quad (4)$$

As the Wigner crystal and Fermi-liquid regions are in series, their effective lengths cover the length of the sample, i.e., $L = l_W + l_F$. The normalized conductivity is then

$$\sigma_{norm}(B) = \frac{\frac{\sigma_W(0)}{\sigma_F(0) + \frac{l_W}{l_F}(0)} - \frac{\sigma_W(B)}{\sigma_F(B) + \frac{l_W}{l_F}(B)}}{\frac{\sigma_W(0)}{\sigma_F(0) + \frac{l_W}{l_F}(0)} - \frac{\sigma_W(\infty)}{\sigma_F(\infty) + \frac{l_W}{l_F}(\infty)}}. \quad (5)$$

Note that, due to the Pomeranchuk effect, the Wigner crystal fraction over the sample depends on in-plane magnetic field as well as temperature [20]. The dependence is explicitly presented in Eq. (5) as $\frac{l_W}{l_F}(B)$.

To understand the kink in B_{sat} versus the total density n_s curve, we need to examine the conductivity given by Eq. (5) for densities slightly smaller than the kink. In this case, the size of the Wigner crystals is small ($l_W \ll l_F$) such that $\frac{\sigma_W}{\sigma_F} \gg \frac{l_W}{l_F}$ and the difference between the normalized conductivity of the Fermi liquid and the normalized conductivity of the whole sample is approximately:

$$\begin{aligned} \frac{\sigma_{norm}^F(B) - \sigma_{norm}(B)}{\sigma_{norm}^F(B)} \approx & \\ & \left[\frac{\sigma_F(0)^2 l_W}{\sigma_W(0) l_F} (0) \left(\frac{1}{\sigma_F(0) - \sigma_F(B)} - \frac{1}{\sigma_F(0) - \sigma_F(\infty)} \right) \right. \\ & \left. - \frac{\sigma_F(B)^2}{\sigma_W(B)} \frac{\frac{l_W}{l_F}(B)}{\sigma_F(0) - \sigma_F(B)} + \frac{\sigma_F(\infty)^2}{\sigma_W(\infty)} \frac{\frac{l_W}{l_F}(\infty)}{\sigma_F(0) - \sigma_F(\infty)} \right] \quad (6) \end{aligned}$$

It can be readily seen from Eq. (6) [or Eq. (5) for that matter] that when $l_W \rightarrow 0$, the normalized conductivity $\sigma_{norm}(B)$ approaches the normalized conductivity of the Fermi liquid [$\sigma_{norm}^F(B)$], as was the case for densities larger than the kink density. This leads to the continuity of B_{sat} versus density at the kink density n_k .

As for the change of the slope of B_{sat} versus density at n_k , we can see from Eq. (6) that, as the density is decreased below n_k , the normalized conductivity starts to deviate from that of the Fermi liquid.

We now show that $\sigma_{norm}^F(B) > \sigma_{norm}(B)$. As discussed in Ref. [20], at low enough temperature and for magnetic fields of the order of saturation magnetic field, the volume fraction of Wigner crystal is of the order of the volume fraction for infinite magnetic field [i.e., $\frac{l_W}{l_F}(B_c) \approx \frac{l_W}{l_F}(\infty)$]. Equation (6) then simplifies to:

$$\begin{aligned} \frac{\sigma_{norm}^F(B) - \sigma_{norm}(B)}{\sigma_{norm}^F(B)} = & \\ & \left[\frac{\sigma_F(0)^2 l_W}{\sigma_W(0) l_F} (0) - \frac{\sigma_F(\infty)^2 l_W}{\sigma_W(\infty) l_F} (\infty) \right] \times \quad (7) \\ & \left[\frac{1}{\sigma_F(0) - \sigma_F(B)} - \frac{1}{\sigma_F(0) - \sigma_F(\infty)} \right] \end{aligned}$$

Here $\sigma_F(B)$ is a decreasing function of B and its value at $B = 0$ is $2\sigma_F(\infty)$. The conductance of Wigner crystals is not sensitive to the applied magnetic field. If the magnetic-field-induced increase of l_W due to the Pomeranchuk effect is not too large [i.e., $\frac{l_W}{l_F}(\infty) < 4\frac{l_W}{l_F}(0)$], which we expect at least for low enough temperatures [20], the value given by Eq.(6) is positive. As a result, $\sigma_{norm}(B) = 0.99$ is achieved at a magnetic field which is less than the saturation magnetic field of the Fermi liquid. This result explains the rapid decrease of B_{sat} versus density at n_k which corresponds to a percolation transition in the mixed phase.

At the lowest densities, the insulating phase covers the whole sample. As a result, the conduction is by individually excited electrons which effectively form a low-density gas. In this limit, the effect of the Zeeman field is to polarize the spin of individual electrons and we can readily show that the slope of the saturation magnetic field versus temperature is the same as for individual electrons.

ACKNOWLEDGMENTS

We are grateful to Teun Klapwijk for providing the split-gate geometry samples that enabled these experiments. We thank Steve Kivelson and Vladimir Dobrosavljevic for valuable discussions and suggestions, and Sergey Kravchenko for his very careful reading of the manuscript. This work was supported by the National Science Foundation Grant No. DMR-1309008 and the Binational Science Foundation Grant No. 2012210. P.G. acknowledges support by NSF EFRI-1542863 and PSC-CUNY Award, jointly funded by The Professional Staff Congress and The City University of New York.

-
- [1] E. Abrahams, P. W. Anderson, D. C. Licciardello, and T. V. Ramakrishnan, *Phys. Rev. Lett.* **42**, 673 (1979).
- [2] S. V. Kravchenko, G. V. Kravchenko, J. E. Furneaux, V. M. Pudalov, and M. D'Iorio, *Phys. Rev. B* **50**, 8039 (1994).
- [3] S. V. Kravchenko, Whitney E. Mason, G. E. Bowker, J. E. Furneaux, V. M. Pudalov, and M. D'Iorio, *Phys. Rev. B* **51**, 7038 (1995).
- [4] S. V. Kravchenko, D. Simonian, M. P. Sarachik, Whitney Mason, and J. E. Furneaux, *Phys. Rev. Lett.* **77**, 4938 (1996).
- [5] T. Okamoto, K. Hosoya, S. Kawaji, and A. Yagi, *Phys. Rev. Lett.* **82**, 3875 (1999).
- [6] S. A. Vitkalov, M. P. Sarachik, and T. M. Klapwijk, *Phys. Rev. B* **64**, 073101 (2001).
- [7] S. A. Vitkalov, H. Zheng, K. M. Mertes, M. P. Sarachik, and T. M. Klapwijk, *Phys. Rev. Lett.* **85**, 2164 (2000).
- [8] E. Abrahams, S. V. Kravchenko and M. P. Sarachik, *Rev. Mod. Phys.* **73**, 251 (2001).
- [9] S. V. Kravchenko and M. P. Sarachik, *Rep. Prog. Phys.* **67**, 1 (2004).
- [10] B. Spivak, S. V. Kravchenko S. A. Kivelson, and X. P. A. Gao, *Rev. Mod. Phys.* **82**, 1743 (2010).
- [11] A. Mokashi, S. Li, B. Wen, S. V. Kravchenko, A. A. Shashkin, V. T. Dolgoplov, and M. P. Sarachik, *Phys. Rev. Lett.* **109**, 096405 (2012).
- [12] D. Simonian, S. V. Kravchenko, M. P. Sarachik and V. M. Pudalov, *Phys. Rev. Lett.* **79**, 2304 (1997).
- [13] V. M. Pudalov, G. Brunthaler, A. Prinz and G. Bauer, *JETP Lett.* **65**, 932 (1997).
- [14] See, for example, K. M. Mertes, D. Simonian, M. P. Sarachik, S. V. Kravchenko and T. M. Klapwijk, *Phys. Rev. B* **60** R5093 (1999).
- [15] Shiqi Li, and M. P. Sarachik, *Phys. Rev. B* **95**, 041301(R) (2017).
- [16] S. A. Vitkalov, H. Zheng, K. M. Mertes, M. P. Sarachik and T. M. Klapwijk, *Phys. Rev. Lett.* **87**, 086401 (2001).
- [17] S. Ilani, A. Yacobi, D. Mahalu and Hadas Shtrikman, *Science* **292**, 1354 (2001).
- [18] S. He and X. C. Xie, *Phys. Rev. Lett.* **80**, 3324 (1998).
- [19] S. Das Sarma, M. P. Lilly, E. H. Hwang, L. N. Pfeiffer, K. W. West, and J. L. Reno, *Phys. Rev. Lett.* **94**, 136401 (2005).
- [20] B. Spivak, *Phys. Rev. B* **67**, 125205 (2003); B. Spivak and S. A. Kivelson, *Phys. Rev. B* **70** 155114 (2004); *Annals of Phys.* **321**, 2071-2115 (2006).
- [21] N. Tenen, A. Yu. Kuntsevich, V. M. Pudalov, and M. Reznikov, *Phys. Rev. Lett.* **109**, 226403 (2012).
- [22] L. A. Morgun, A. Yu. Kuntsevich and V. M. Pudalov, *Phys. Rev. B* **93**, 235145 (2016).
- [23] Matthias Baenninger, Arindam Ghosh, Michael Pepper Harvey E. Beere, Ian Farrer and David A. Ritchie, *Phys. Rev. Lett.* **100**, 016805 (2008).
- [24] Yigal Meir, *Phys. Rev. Lett.* **83**, 3506 (1999).
- [25] M. J. Manfra, E. H. Hwang, S. Das Sarma, L. N. Pfeiffer, K. W. West and A. M. Sergent, *Phys. Rev. Lett.* **99**, 236402 (2007).
- [26] J. Yoon, C. C. Li, D. Shahar, D. C. Tsui, and M. Shayeghan, *Phys. Rev. Lett.* **84**, 4421 (2000).
- [27] A. A. Shashkin, S. V. Kravchenko, V. T. Dolgoplov and T. M. Klapwijk, *Phys. Rev. Lett.* **87**, 086801 (2001).
- [28] V. M. Pudalov, G. Brunthaler, A. Prinz and G. Bauer, *Phys. Rev. Lett.* **88**, 076401 (2002).
- [29] Y. Tsui, S. A. Vitkalov, M. P. Sarachik and T. M. Klapwijk, *Phys Rev B* **71**, 033312 (2005).
- [30] K. Lai, W. Pan, D. C. Tsui, S. A. Lyon, M. Muhlberger, and F. Schaffler, *Phys. Rev. B* **72**, 081313(R) (2005).
- [31] Dragana Popovic, in *Conductor Insulator Quantum Phase Transitions*, edited by Vladimir Dobrosavljevic, Nandini Trivedi and James M. Valles, Jr. (Oxford University Press, Oxford, UK, 2012), p. 256.
- [32] I. Shlimak, A. Butenko, D. I. Golosov, K. J. Friedland and S. V. Kravchenko, *Eur. Phys. Lett.* **97**, 37002 (2012).
- [33] T. M. Lu, L. Sun, D. C. Tsui, S. Lyon, W. Pan, M. Muhlberger, F. Schaffler, J. Liu and Y. H. Xie, *Phys Rev. B* **78**, 233309 (2008). (2018).
- [34] V. M. Pudalov, A. Yu. Kutsevich, M. E. Gershenson, I. S. Burmistrov and M. Reznikov, *Phys. Rev. B* **98**, 155109 (2018).
- [35] Scott Kirkpatrick, *Rev. Mod. Phys.* **45**, **574**, 574-588 (1973).
- [36] Interestingly, transport evidence for quantum electron crystallization in silicon MOSFETs has recently been reported by P. Brussarski, S. Li, S. V. Kravchenko, A. A. Shashkin and M. P. Sarachik, *Nature Comm.* **9** 3803 (2018).